

Learning to Navigate: Exploiting Deep Networks to Inform Sample-Based Planning During Vision-Based Navigation

Justin S. Smith¹, Jin-Ha Hwang¹, Fu-Jen Chu¹, and Patricio A. Vela¹

Abstract—Recent applications of deep learning to navigation have generated end-to-end navigation solutions whereby visual sensor input is mapped to control signals or to motion primitives. The resulting visual navigation strategies work very well at collision avoidance and have performance that matches traditional reactive navigation algorithms while operating in real-time. It is accepted that these solutions cannot provide the same level of performance as a global planner. However, it is less clear how such end-to-end systems should be integrated into a full navigation pipeline. We evaluate the typical end-to-end solution within a full navigation pipeline in order to expose its weaknesses. Doing so illuminates how to better integrate deep learning methods into the navigation pipeline. In particular, we show that they are an efficient means to provide informed samples for sample-based planners. Controlled simulations with comparison against traditional planners show that the number of samples can be reduced by an order of magnitude while preserving navigation performance. Implementation on a mobile robot matches the simulated performance outcomes.

I. INTRODUCTION

Contemporary machine learning (ML) algorithms demonstrate the potential to provide end-to-end learning such that navigation tasks can be replaced with black box image-to-control or image-to-action mappings [1], [2]. This data-driven approach is inline with—but on a path to supercede—traditional (manually engineered) reactive navigation strategies. The idea behind ML methods is that the underlying learner, today usually a deep network, implicitly learns structural models of the world within its internal representation. These implicit structural models are then encoded in the feature vector output of the network and support effective decision making at the output end, following the incorporation of a shallow learner.

The traditional deliberative, or global, navigation pipeline is heavily model based (in the sense that it requires models of the robot and the world) and is at odds with end-to-end machine learning approaches. Several ML-navigation based papers further conclude that it is best to fuse their algorithms with higher level planners to overcome the short-term, greedy nature of ML-navigation [2], [3]. One structural issue with doing so is that typical end-to-end systems are often not meant to consider higher level planning actions, thus there is no obvious procedural strategy for achieving the desired recommendation. An exception being ML-strategies

that explicitly incorporate the task [3], or that learn motion primitives [4]. The latter can be concatenated with a higher level planner. Additional work is needed though to align the motion primitive control decisions with the global goal.

In this paper, we explore the standard ML pipeline used for end-to-end navigation and demonstrate that it is not well suited to incorporation into the traditional, closed-loop, goal-directed navigation pipeline. Furthermore, since traditional global navigation approaches involve exhaustive or highly sampled search, their performance relative to ML-methods should be considered as upper bounds. Taking a systems view of vision-based navigation, we propose sensible modifications to ML-based navigation methods so that they are more compatible with the traditional goal-directed navigation stack. Importantly, the input/output function learnt must be altered to consider down-stream use of the ML output. Implementing the modified ML-driven approaches in controlled simulations we show that a planning-aware ML-based approach to navigation can indeed provide comparable performance to more global or exhaustive approaches while reducing the trajectory search space. The ML-based module effectively acts as a data-driven sampling heuristic for minimizing the trajectory search and providing presumably high quality navigation directions. The resulting planner leverages learning where learning excels, and relies on model-based strategies where they excel.

A. Related Work

Due to the extensive literature and history of research efforts on planning, this review of related work focuses primarily on contemporary learning-based approaches to navigation. It is presumed that the reader has some familiarity with planning in general [5].

Collision-free navigation requires processing sensor measurements to understand or infer the local scene geometry, then making a navigation decision based on both the scene geometry and the global goal points. For mobile robots with monocular cameras, depth information must be inferred from the sensing time signal. As an input/output mapping, ML has shown success in recovering good estimates of scene structure for navigation purposes [6], [7], [8]. The ML block generates missing information for decision making.

Others propose an end-to-end process, whereby image to control decisions are learnt instead [1], [2]. In the cases where expert demonstration is employed, it is not clear that the expert’s motives for the control decisions necessarily translate to desirable navigation choices given the mobile robot’s goals. When the control objective is clear, as in

*This work supported in part by NSF Awards #1400256 and #1605228.

¹J.S. Smith, J. Hwang, F.J. Chu, and P.A. Vela are with the School of Electrical and Computer Engineering and the Institute for Robotics and Intelligent Machines, Georgia Institute of Technology, Atlanta, GA 30308, USA. {jssmith, jhwang44, fujenchi, pvela}@gatech.edu

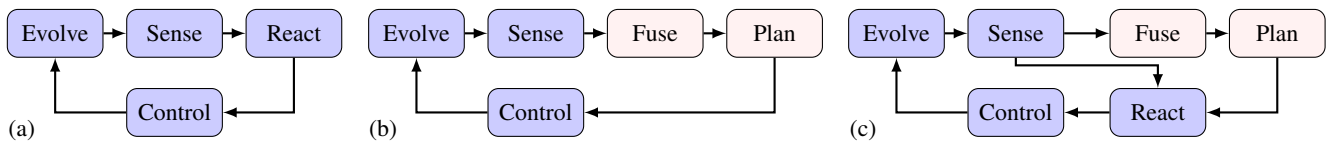


Fig. 1: Block diagram of (a) local/reactive; (b) global/deliberative; and (c) mixed navigation pipelines.

stabilization, then the image to control mapping is effectively injective, thereby reducing mismatch between implicit information contained in the training set and the explicit goal [9]. Another issue that arises with many end-to-end methods is that the underlying strategy is functionally a regressor [10]. For navigation, which is non-convex due to the topological splits that occur in trajectory space, regression may not be the best choice. Similar problems may arise for methods that learn motion primitives for specific scenarios [4], as a particular motion primitive may be biased towards one topological instance of a reaction from a set of potential reactions. The bias may undermine the global objective.

The work in [3] is one of the first to consider the goal state within end-to-end training, which involves laser scans and relative target waypoints as input and steering commands as output. However, their system still requires human intervention to correct for local minima since it is not linked to higher level planning. It is not clear how successful the system is at autonomous operation relative to the global objective since baseline comparison against standard methods is not performed.

An intermediate family of ML-navigation methods convert the image into actionable information (or affordance states), such as local structural information useful for driving along roadways [11] (e.g., distance to vehicles, lane locations, lane marker relative offsets, etc.). Another example learns to identify forest trails for navigation guidance [12]. The output states are used to then generate a navigation decision. The target application is usually a restricted form of navigation.

When input imagery is too novel or reflects extreme imaging conditions, then ML-models may fail at the trained task. Detecting failure, or the potential of failure, can itself be cast into a learning framework to thereby supervise the online end-to-end ML controller [13], [14]. In [15], the supervisor is an autoencoder whose reconstruction should match the scene. Failure to reconstruct the input image indicates an out-of-sample situation requiring a fall-back plan.

Within the area of Reinforcement Learning (RL), it is common to learn image-to-action mappings, usually in the context of video games [16], [17], [18], [19], [20]. By virtue of an existing reward function, the methods learn task-oriented behavior. Though the imagery may be quite diverse, the underlying task domain is usually limited in scope relative to the general task of navigation, and the approaches seek a slightly different purpose from the one stated here. Though [21], [22] concern navigation and even consider specific task-based objectives, the aim of the research is to demonstrate implicit learning of the environment from imagery based on repeated trials within the environment. Changing the environment requires further rounds of training.

B. Robotic Navigation Systems

Figure 1 depict three varieties of navigation pipelines. The majority of ML-based navigation methods operate at the reactive level, Figure 1a, whereas some of the task-based and game-based methods operate as per Figure 1b for the case of a given, fixed environment. In these instances, novel or altered environments require additional training to re-learn. It is not clear that they could ever really operate at the deliberative or global level for general purpose navigation tasks as the underlying model complexity is quite large. None of the methods described operate as per Figure 1c. This paper is concerned with the closed-loop consequences of traditional end-to-end ML pipelines while exploring means to achieve a fused system with ML for the local/reactive planner and a model-based approach for the global/deliberative planner.

As foundational elements for our local/global fusion, we utilize traditional methods that work at the local and global levels, such as dynamic window approach (DWA) [23], elastic bands (EB) [24], and timed elastic bands (TEB) [25], and their existing ROS implementations. Thus, the investigation does not seek to propose new planning strategies, nor new learning architectures, but rather it seeks to investigate how to effectively integrate ML-based approaches into existing navigation pipelines. The remainder of this paper covers the deep learning strategy, the planning integration, and test results from simulation and real-world operation.

II. DEEP LEARNING

The AlexNet [26] deep convolutional neural network serves as the foundation for our model. To facilitate learning from few training samples, pre-training of the network involves using the ImageNet dataset [27] and its associated training task. We replace the final layer of the network with a shallow, single-layer learner (described in II-C). Several learning tasks are explored, including the traditional approaches from the literature: control action regression (continuous output), and control action classification (discrete output). Prior to explaining the different output spaces, we first describe the common aspects of the training methodology.

A. Generating Data Samples

As is rapidly becoming the standard, we train with simulated data [2], [3], [8], [21]. We use the Gazebo simulator to model our robot and a depth sensor in various scenarios.

Capturing scenes: Three (roughly cylindrical) trash cans are randomly (uniformly) placed in a rectangular region in front of the robot. The region extends from 1 to 5 meters in front of the robot and 3 meters to either side. Not all of the region can be seen by the depth sensor, resulting in some scenarios with

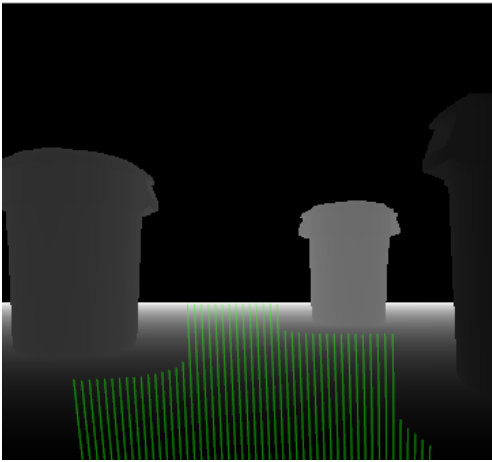


Fig. 2: Training Sample: Depth image with non-colliding trajectory poses overlaid in green.

fewer than 3 trash cans in them. A depth image is captured by the depth sensor then decimated by 4, resulting in image samples with dimensions 140x120.

Generating Trajectories: Using the trajectory generation and collision-checking approaches of [28], we evenly sample 51 robot departure angles in the range $[-0.4, .4]$ radians. It involves converting the departure angle into a feasible trajectory, generating a sequence of poses along the trajectory, then checking each pose for collisions. The non-colliding poses per departure angle reveal how far the robot can safely travel for each departure angle (see Figure 2). This approach will implicitly encode the geometry of the robot relative to the geometry of the world, as the collision checking employs a solid model of the robot. A robot with different geometry, motion kinematics/dynamics, and dynamic constraints would need this training phase to incorporate those models. Our model was the TurtleBot 2 mobile robot whose constraints are obtained from the manufacturer’s datasheet.

Retaining Final Pose: We retain the last non-colliding pose of each trajectory tested. The pose information is later converted into the appropriate output signal based on the desired output space. The task metric employed for a given learning scenario dictates how to use the stored final pose information.

Generating Dataset Statistics: We calculate the the per-pixel means and standard deviations for the dataset and save them with the rest of the data. The statistics are used to normalize samples for training and inference.

B. Learning the Model

Implement and training of the model is done with TensorFlow; in particular, using the Adam optimizer with a learning rate of .001. Training is performed with a batch size of 600 on an NVidia 1070GTX GPU. Training images are uniformly sampled from dataset. After each epoch, the model is run against a separate testing set. When a sample is selected either for training or for testing, the image is normalized and resized to match the expected dimensions of AlexNnet

(227x227). The result is then copied across 3 channels (the original network was intended for RGB images).

For classification-based output spaces, the loss function is cross entropy with logits. For regression-based output spaces, the loss function is the L_2 -norm. Training ends when the loss levels off; this occurs within 500 iterations (~ 35 epochs).

C. Input/Output Mappings

The deep network model is intended to inform the trajectory selection or search process by using depth images as inputs. In this work, we use the same family of trajectories as in our prior work [28]. These trajectories are parameterized by the initial robot velocity and a departure angle. As a simplification, we assume a constant forward velocity. Since these trajectories only involve strong rotations for brief periods, it is a reasonable assumption.

We implement three versions with different output spaces. The first two represent implementations reported in the literature. In all of the versions, the intermediate label representation is the Euclidean distance from the body frame origin to the end pose of each departure angle (relative to the body frame).

1) *Regression:* In this version, the last layer of the AlexNet model is replaced with a 1024x1 fully connected layer with no ReLU. The output of this model is a departure angle. The correct output is the departure angle corresponding to the greatest distance. In one version, the regressor was goal-agnostic, in another it is goal-informed.

2) *Best Angle Classifier:* In this version, the last layer of the AlexNet model is replaced with a 1024x51 fully connected layer with ReLU. The 51 output values represent the confidences of the corresponding departure angle being the correct one. The winning class is the departure angle with the greatest distance. In this strategy, there is competition amongst the classifiers.

3) *Collision-free Angles Classifier:* In this version, the last layer of the AlexNet model is replaced with a 1024x102 fully connected layer with ReLU, with the output reshaped to 51x2. After applying softmax to the last dimension, each 1x2 pair represents the positive and negative confidences of a departure angle being non-colliding. A departure angle is classified as non-colliding if it’s distance is greater than or equal to 4.0m, the approximate effective range of a Kinect. In contrast to the *Best Angle Classifier*, this version yields a family of independent (non-competing) 51 binary classifiers.

The last classifier is motivated by our experiences with the first three models trained (the two regression and *best angles* classifier), which did not have strong performance (see Section IV). Evaluating trajectories for collisions is computationally costly, therefore we seek to reduce the number of trajectories that we need to evaluate in order to find a satisfactory one. The purpose of the model is to learn a mapping between depth images and departure angles. The model should not dictate which departure angle to use, however, as that would leave no room for higher level planning systems to operate. Rather, it should indicate which

departure angles are likely to yield good (i.e. non-colliding) trajectories.

III. PLANNING FRAMEWORK

At every local path-planning invocation, the depth image is provided to the trajectory generator to generate an output. For the ML-navigation strategies that lead to a single outcome, the high-level planner plays little to no role. For all other strategies, the samples get passed to a trajectory evaluator that then selects the locally optimal choice. We incorporate Dynamic Window Approach, Elastic Band, and Timed Elastic Band local planner options within a global planning framework using the ROS `move_base` package. These planners served as the baseline planner approaches for the comparison with ML-integrated global/local planners.

The ROS path planning and navigation stack supports several cost functions to guide the navigation. With respect to the current position and orientation of the robot, the scoring functions included in our navigation objective function are the following:

- 1) Goal Heading: robot directed relative to goal direction;
- 2) Path Heading: path keeps the robot nose on the nose path;¹
- 3) Path Distance: path proximity to to global path;
- 4) Goal Distance: path leads robot closer to goal; and
- 5) Obstacle Cost: path avoids obstacles.

They score the sampled trajectory according to the preferences stated above. The first two score the orientation component of the path, the second two score the position, and the last embodies obstacle avoidance. Once the trajectory that the robot should follow is selected, the trajectory is then converted into velocity commands and executed in the low-level trajectory controller. The navigation system follows the path until the next planning stage. For laser scan-based local planners that store obstacles in a Cartesian occupancy grid, re-planning is triggered every 1 second. The laser scan data is simulated from a single horizontal line from the depth image. Cartesian grid planners with this laser scan data will inherit any field-of-view limitations associated to the depth image. The perception space local planners [28] re-plan when the robot achieves 60% of the planned trajectory from the last planning stage or if it detects a collision along the predicted path (occurs with dynamic obstacles).

Unlike traditional learning based approaches that are usually trained without awareness of the goal state, our system implemented two additional methods on the top of trajectory selection algorithm to find both locally and globally optimal candidates. One is a “to-goal” approach where the departure angle that points most directly to the goal is added in addition to the top k departure angles from the model. Another is “Gaussian-based goal bias” approach which biases trajectory selection based on the relative position of the goal. It weights the raw classification confidence scores by a Gaussian prior

¹The “nose” is a virtual point ahead of the robot that exploits differential flatness to simplify the feedback control signal. The planned path also has such a point. It implicitly encodes the path tangent.

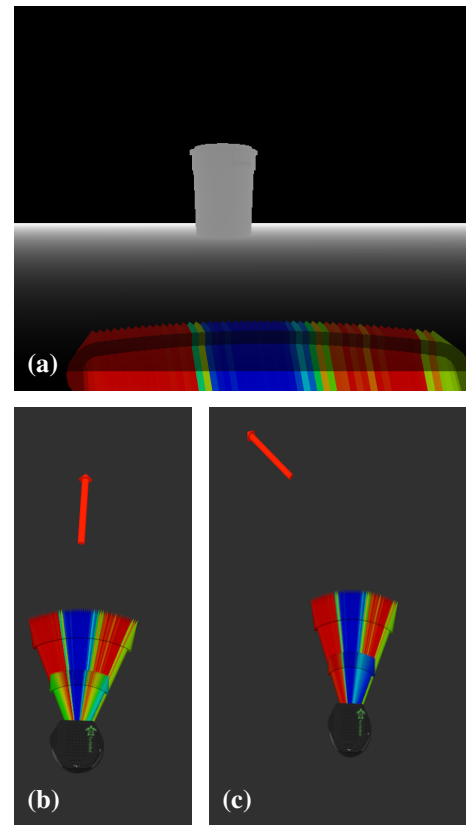


Fig. 3: Sample scenario with a barrel straight ahead. (a) Depth image shown with color coded rays indicating the classifier confidence of each angle. Red denotes highest confidence and blue lowest. (b) Depiction of goal influence on confidence. The longer vectors are the original confidences, while the shorter vectors of the inner wedge of rays has the goal-influenced confidences. For a straight ahead goal the left and right splits are equally high in the directions that minimize path length. (c) Depicts the same for a goal to the left. Now the confidences are biased towards the goal and there is no left/right split for the goal-influenced confidences.

centered on the departure angle that would point directly to the goal. In Figure 3, long arrows represent unbiased trajectory candidates while the shorter arrows indicate the weighted values.

IV. EXPERIMENTAL EVALUATION

To evaluate the quality of the overall ML-enhanced navigation pipelines, we run the vision-based navigation system in Gazebo-simulated environments and on an actual mobile robot (Turtlebot). Simulation serves to create highly repeatable and consistent test conditions for evaluating a variety of planning implementations.

In what follows, we do not report the results for the regression-based approaches. Both the goal-agnostic and the goal-informed regression approaches perform poorly and can not navigate without collision, in contrast to [10] who report success at a regression approach, as well as [3] whose method is goal-informed. We believe differences in training

sets may be responsible for the differences in performance. Our training scenes involve randomly placed obstacles in the field of view and simulate only one instance in time, whereas those from [10] appear to be mostly corridor images that arise from actually executing a path. Our learnt model would have no notion of a corridor in its internal representation. The model in [3] is trained in a sparser environment with large obstacles using navigation commands from a global planner. Topologically distinct trajectory splits would not be as frequently observed in those models.

A. Barrel Forest

The first battery of navigation tests in a simulated environment involves positioning barrels in random locations within a $10 \times 6m^2$ world where the robot’s goal is to travel 8 meters forward. the number of barrels randomly spawned is set to 3, 5, and 7 across three sets of trials. For each quantity of barrels, 50 scenes are created. For every instantiated scene, we initialize the navigation pipeline with each of the following local planners:

- 1) Dynamic Window Approach
- 2) Elastic Band
- 3) Timed Elastic Band
- 4) Learning PiPS + To-Goal
- 5) Learning PiPS + Goal-Biased
- 6) Learning Cartesian + To-Goal
- 7) Learning Cartesian + Goal-biased
- 8) Learning Naive + Goal-Biased

where PiPS is the perception space planner [28]. The last planner tested is the traditional end-to-end planner with a discrete steering space and a winner-takes-all multi-class classifier (sometimes called the “naive” planner as it represents a typical first pass solution to the end-to-end learning problem, after regression). However, it also includes goal biasing. The objective of each task is to simply move from one end of the world to the other end without crashing.

The first three approaches described above use traditional exhaustive trajectory search, creating 200 trajectory candidates at each replanning phase. The learning-based approaches generate trajectories using the five departure angles with the highest confidences. For the Naive approach, the trajectory with the highest confidence is executed without scene analysis (i.e. no collision checking). In order to test the original quality of the trajectory selection strategies, we disable the recovery behavior performed by the global planner when the local planner reports being stuck.

1) *Controller Comparison:* Figure 4 graphs empirical results for the Barrel forest navigation task. Recall that performance should not be perfect due to (1) disabling of the local-minima recovery behavior and (2) field-of-view limitations that mean the robot might turn into an unseen object. In this experiment, the TEB local planner consistently has the highest success rate while the Naive controller has the lowest. However, the experiment shows that path-planning using only five ML-predicted trajectories per planning stage can achieve a success rate close to traditional exhaustive

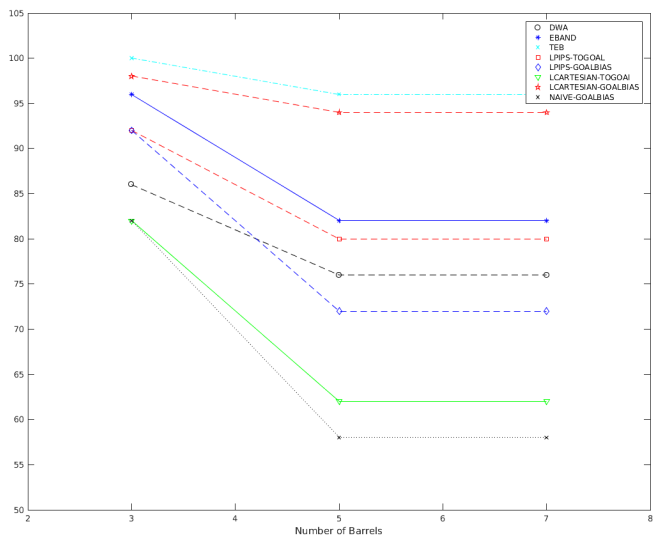


Fig. 4: Barrel Forest Success Rate

TABLE I: Success Rate vs Trajectory Candidate Quantities

# candidate trajectories	Success Count	Rate
2	29	58%
3	36	72%
5	38	76%
7	39	78%

trajectory search-based planners. The ML methods sample only $\frac{1}{40}$ as many trajectories as the exhaustive searchers.

The ML Cartesian planner with Gaussian goal biasing performs only 2% worse than TEB and outperforms EB and DWA. Learning PiPS with Gaussian goal biasing outperformed DWA. The difference in performance is that the Cartesian planners incorporate some memory in the local cost-map, whereas PiPS has no memory. It runs a higher risk of turning back into objects that leave the field of view when being passed. Adding memory should improve performance.

2) *Trajectory number comparison:* Next, we test the impact of varying the number of trajectories generated by the ML planners. The number of barrels is fixed to 5 while the number of trajectories sampled is set to 2, 3, 5, 7 across four trial sets. There are 50 trial scenes with randomly spawned barrels. To increase the difficulty of the scenario, the barrel spawn zone is made smaller, thereby increasing the density of the “barrel forest.” We use the Learning Cartesian planner with Gaussian Goal-biasing since it has the the best performance of the ML approaches we are testing. As in the previous experiment, we disable recovery behaviors. From Table I, the experimental results show that the number of trajectory candidates provided by the learning-based model does not have a significant impact on success rate as long as more than three candidates are provided into the evaluation.

We examine the failure cases to determine their sources. In some of these cases, the classifier failed to return valid trajectories when an exhaustive search would have succeeded. These cases could be resolved by one of following approaches: switching to an exhaustive search when the

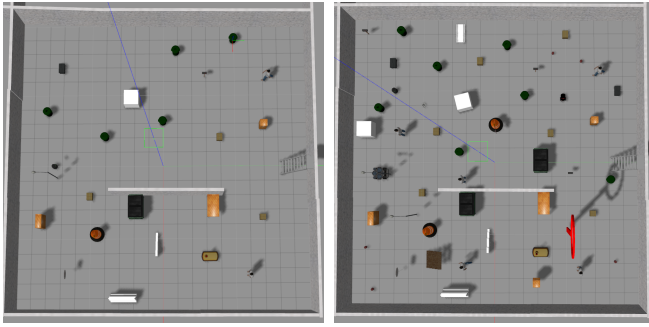


Fig. 5: Sparse (left) and dense (right) sector worlds.

ML approach fails, or replanning the global path using the information gathered from local planners.

Exhaustive searching should be avoided if possible, but can always be tried as a fallback approach. In order to test the second approach, we rerun the 11 failure cases from the scenario with 7 candidate trajectories with the recovery behavior enabled. In 6 out of 11 times, a new global plan is found that successfully reaches the goal. The remaining 5 cases fail due to the recovery behavior being tailored to laser scan models. The robot turns 360 degrees and returns to face the same scene. A more standard laser scanner would most likely provide better information than the depth limited kinect scanner. One option may be to create a new recovery behavior for visual navigation strategies.

B. Sector World

We also test our approach in environments that are divided into sectors and populated with an assortment of objects. The two test environments are depicted in Figure 5, one sparsely populated and one more densely populated with more diverse object categories (recall that only garbage cans were in the training set). The object positioning remains static while the start and goal sectors are randomly selected for each test. The objective of this experiment is to navigate from the start zone and travel to the goal sector without crashing. In this experiment we compare the best PiPS approach (Learning PiPS + To Goal) to the best traditional approach (TEB). For both worlds, we test 35 navigation sector-pairs, again with the recovery behavior disabled. The results are in Table II.

The ML-based trajectory generation strategy outperforms the exhaustive trajectory TEB local planner for the easy sector world. In denser environment, the success rate decreased 23% for the ML planner and increased about 3.5% for the TEB planner. The less than perfect completion rate for both approaches reinforces the well-accepted observation that local planners need augmentation by global planners with recovery behaviors, as well as the need to consider the full navigation pipeline when creating and evaluating ML-based image-to-decision navigation methods.

C. Real World Implementation

Lastly, we implemented our ML-based planner module on a Turtlebot 2 equipped with a laptop. Given a goal and a

known starting position, the robot is able to navigate through obstacles with only 5 ML-generated trajectory candidates. In 13 of the 15 tests, navigation from start to goal is successful. For 2 of the 15 cases, the Turtlebot collides with objects located just outside the field of view. Figure 6 consists of overhead views of one navigation scenario. The Turtlebot starts off screen at the upper-right (just past the barely visible white angle marker) and is directed to travel to another off-screen location at the lower-left of the image, offscreen. The start and final positions are chosen such that following the straight line path results in collisions. In the last image one can see how closely the PiPS planner tends to get to obstacles when passing them.

V. CONCLUSION

This paper explores the behavior of typical end-to-end machine learning based navigation strategies under controlled simulation conditions, as well as proposes a revised training and trajectory generation method based on the outcomes of the strategies. While demonstrating success at collision-free wandering in natural, real-world environments, the traditional ML algorithms perform poorly when faced with a goal-directed navigation task. By modifying the input/output mapping, adjusting the training data provided and its evaluation criteria, and incorporating well established goal-directed modifications to the planning pipeline, a deep learning based modification to existing navigation stacks is described. In controlled conditions, the proposed deep learning navigation strategy is shown to operate as effectively as commonly used methods in the robotics community. Furthermore, the number of trajectories needed to find a path is significantly reduced.

Further work is needed to resolve the issues that arise from the limited field of view associated to dense visual sensors. One solution would be to incorporate additional memory within the local planner, whereas another would be to modify the model and training procedure to consider the time history of decisions in order to implicitly learn to create a buffer away from obstacles when passing them.

REFERENCES

- [1] S. Ross, N. Melik-Barkhudarov, K. Shankar, A. Wendel, D. Dey, J. Bagnell, and M. Hebert, "Learning monocular reactive uav control in cluttered natural environments," in *Proceedings of IEEE International Conference on Robotics and Automation*, 2013, pp. 1765–1772, karlsruhe, Germany.
- [2] F. Sadeghi and S. Levine, "Cad²rl: Real single-image flight without a single real image," in *Proceedings of Robotics: Science and Systems*, 2017.
- [3] M. Pfeiffer, M. Schaeuble, J. Nieto, R. Siegwart, and C. Cadena, "From perception to decision: A data-driven approach to end-to-end motion planning for autonomous ground robots," in *Proceedings of IEEE International Conference on Robotics and Automation*, Singapore, 2017, pp. 1527–1533.
- [4] T. Zhang, G. Kahn, S. Levine, and P. Abbeel, "Learning deep control policies for autonomous aerial vehicles with mpc-guided policy search," in *Proceedings of IEEE International Conference on Robotics and Automation*, 2016, pp. 528–535, stockholm, Sweden.
- [5] S. M. LaValle, *Planning algorithms*. Cambridge university press, 2006.
- [6] K. Bipin, V. Duggal, and K. M. Krishna, "Autonomous navigation of generic monocular quadcopter in natural environment," in *Proceedings of IEEE International Conference on Robotics and Automation*, 2015, pp. 1063–1070.

TABLE II: Experimental results for Sector World.

	World A (Sparse)		World B (Dense)	
	Success Rate (%)	Avg. Time (s)	Success Rate (%)	Avg. Time (s)
LPIPS-ToGoal	93.33	57.55	70	66.02
TEB	86.56	55.8	90	63.41

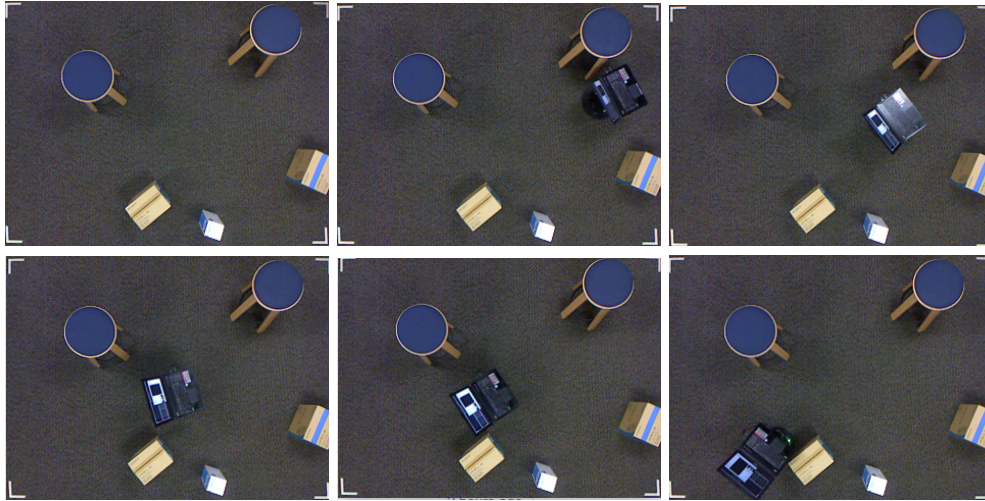


Fig. 6: Overhead snapshots of Turtlebot navigating an obstacle course (chronologically: from top left to top right, then bottom left to bottom right).

- [7] K. Lamers, S. Tijmons, C. De Wagter, and G. de Croon, "Self-supervised monocular distance learning on a lightweight micro air vehicle," in *Proceedings of the IEEE International Conference on Intelligent Robotic and Systems*, Daejeon, South Korea, 2016, pp. 1779–1784.
- [8] J. Michels, A. Saxena, and A. Ng, "High speed obstacle avoidance using monocular vision and reinforcement learning," in *Proceedings of International Conference on Machine Learning*, 2005.
- [9] H. van Hoof, N. Chen, M. Kar, P. van der Smagt, and J. Peters, "Stable reinforcement learning with autoencoders for tactile and visual data," in *Proceedings of the IEEE International Conference on Intelligent Robotic and Systems*, Daejeon, South Korea, 2016, pp. 3928–3934.
- [10] L. Tai, S. Li, and M. Liu, "Autonomous exploration of mobile robots through deep neural networks," *International Journal of Advanced Robotic Systems*, vol. 14, no. 4, 2017.
- [11] C. Chen, A. Seff, A. Kornhauser, and J. Xiao, "DeepDriving: Learning affordance for direct perception in autonomous driving," in *IEEE International Conference on Computer Vision*, Santiago, Chile, 2015, pp. 2722–2730.
- [12] A. Giusti, J. Guzzi, D. C. Cireşan, F. L. He, J. P. Rodríguez, F. Fontana, M. Faessler, C. Forster, J. Schmidhuber, G. D. Caro, D. Scaramuzza, and L. M. Gambardella, "A machine learning approach to visual perception of forest trails for mobile robots," *IEEE Robotics and Automation Letters*, vol. 1, no. 2, pp. 661–667, 2016.
- [13] S. Daffry, S. Zeng, J. A. Bagnell, and M. Hebert, "Introspective perception: Learning to predict failures in vision systems," in *Proceedings of the IEEE International Conference on Intelligent Robotic and Systems*, 2016, pp. 1743–1750.
- [14] D. M. Saxena, V. Kurtz, and M. Hebert, "Learning robust failure response for autonomous vision based flight," in *Proceedings of IEEE International Conference on Robotics and Automation*, Singapore, 2017, pp. 5824–5829.
- [15] C. Richter and N. Roy, "Safe visual navigation via deep learning and novelty detection," in *Proceedings of Robotics: Science and Systems*, 2017.
- [16] X. Guo, S. Singh, H. Lee, R. Lewis, and X. Wang, "Deep learning for real-time atari game play using offline Monte-Carlo tree search planning," in *Advances in Neural and Information Processing Systems*, 2014.
- [17] M. Kempka, M. Wydmuch, G. Runc, J. Toczek, and W. Jaskowski, "ViZDoom: A Doom-based AI research platform for visual reinforcement learning," in *IEEE Conference on Computational Intelligence and Games*, Santorini, Greece, 2016.
- [18] Y. Liang, M. Machado, E. Talvitie, and M. Bowling, "State of the art control of atari games using shallow reinforcement learning," in *Proc. of International Conference on Autonomous Agents & Multiagent Systems*, Singapore, Singapore, 2016, pp. 485–493. [Online]. Available: <http://dl.acm.org/citation.cfm?id=2936924.2936996>
- [19] R. Mottaghi, H. Bagherinezhad, M. Rastegari, and A. Farhadi, "Newtonian image understanding: Unfolding the dynamics of objects in static images," in *Proceedings IEEE Conference on Vision and Pattern Recognition*, Las Vegas, NV, 2016, pp. 3521–3529.
- [20] J. Wu, I. Yildirim, J. Lim, W. Freeman, and J. Tenenbaum, "Galileo: Perceiving physical object properties by integrating a physics engine with deep learning," in *Advances in Neural and Information Processing Systems*, 2015.
- [21] P. Mirowski, R. Pascanu, F. Viola, H. Soyer, A. Ballard, A. Banino, M. Denil, R. Goroshin, L. Sifre, K. Kavukcuoglu, D. Kumaran, and R. Hadsell, "Learning to navigate in complex environments," in *Proceedings of International Conference on Learning Representations*, Toulon, France, 2017.
- [22] Y. Zhu, R. Mottaghi, E. Kolve, J. J. Lim, A. Gupta, L. Fei-Fei, and A. Farhadi, "Target-driven visual navigation in indoor scenes using deep reinforcement learning," in *Proceedings of IEEE International Conference on Robotics and Automation*, 2017, pp. 3357–3364.
- [23] D. Fox, W. Burgard, and S. Thrun, "The dynamic window approach to collision avoidance," *Robotics Automation Magazine, IEEE*, vol. 4, no. 1, pp. 23–33, Mar 1997.
- [24] S. Quinlan and O. Khatib, "Elastic bands: connecting path planning and control," in *[1993] Proceedings IEEE International Conference on Robotics and Automation*, May 1993, pp. 802–807 vol.2.
- [25] C. Rösmann, W. Feiten, T. Wösch, F. Hoffmann, and T. Bertram, "Efficient trajectory optimization using a sparse model," in *2013 European Conference on Mobile Robots*, Sept 2013, pp. 138–143.
- [26] A. Krizhevsky, I. Sutskever, and G. E. Hinton, "Imagenet classification with deep convolutional neural networks," in *Advances in neural information processing systems*, 2012, pp. 1097–1105.
- [27] J. Deng, W. Dong, R. Socher, L.-J. Li, K. Li, and L. Fei-Fei, "Imagenet: A large-scale hierarchical image database," in *Computer Vision and Pattern Recognition, 2009. CVPR 2009. IEEE Conference on*. IEEE, 2009, pp. 248–255.
- [28] J. S. Smith and P. Vela, "Pips: Planning in perception space," in *Robotics and Automation (ICRA), 2017 IEEE International Conference on*. IEEE, 2017, pp. 6204–6209.